Parasitology International 65 (2016) 196–204

Contents lists available at ScienceDirect

Parasitology International

journal homepage: www.elsevier.com/locate/parint

Characterization of *TcCYC6* from *Trypanosoma cruzi*, a gene with homology to mitotic cyclins

María Agostina Di Renzo [a], Marc Laverrière [b,1], Sergio Schenkman [c], Diana Patricia Wehrendt [a], María Teresa Tellez-Iñón [a], Mariana Potenza [a,*]

[a] Instituto de Investigaciones en Ingeniería Genética y Biología Molecular "Dr. H.N. Torres", INGEBI-CONICET, Vuelta de Obligado 2490 (C1428ADN), Buenos Aires, Argentina
[b] Instituto de Investigaciones Biotecnológicas IIB-INTECH, Universidad Nacional de San Martín - CONICET, Buenos Aires, Argentina
[c] Departamento de Microbiologia, Imunologia e Parasitologia, Universidade Federal de São Paulo, Rua Pedro de Toledo 669 6andar (SP 04039-032), São Paulo, Brazil

ARTICLE INFO

Article history:
Received 29 June 2015
Received in revised form 14 December 2015
Accepted 16 December 2015
Available online 17 December 2015

Keywords:
Cell cycle
Cyclin
Destruction box
Trypanosoma cruzi

ABSTRACT

Trypanosoma cruzi, the etiologic agent of Chagas disease, is a protozoan parasite with a life cycle that alternates between replicative and non-replicative forms, but the components and mechanisms that regulate its cell cycle are poorly described. In higher eukaryotes, cyclins are proteins that activate cyclin-dependent kinases (CDKs), by associating with them along the different stages of the cell cycle. These cyclin–CDK complexes exert their role as major modulators of the cell cycle by phosphorylating specific substrates. For the correct progression of the cell cycle, the mechanisms that regulate the activity of cyclins and their associated CDKs are diverse and must be controlled precisely. Different types of cyclins are involved in specific phases of the eukaryotic cell cycle, preferentially activating certain CDKs. In this work, we characterized *Tc*CYC6, a putative coding sequence of *T. cruzi* which encodes a protein with homology to mitotic cyclins. The overexpression of this sequence, fused to a tag of nine amino acids from influenza virus hemagglutinin (*Tc*CYC6-HA), showed to be detrimental for the proliferation of epimastigotes in axenic culture and affected the cell cycle progression. In silico analysis revealed an N-terminal segment similar to the consensus sequence of the destruction box, a hallmark for the degradation of several mitotic cyclins. We experimentally determined that the *Tc*CYC6-HA turnover decreased in the presence of proteasome inhibitors, suggesting that *Tc*CYC6 degradation occurs via ubiquitin–proteasome pathway. The results obtained in this study provide first evidence that *Tc*CYC6 expression and degradation are finely regulated in *T. cruzi*.

© 2015 Elsevier Ireland Ltd. All rights reserved.

1. Introduction

Trypanosoma cruzi is the etiological agent of Chagas's disease, an endemic illness affecting mainly the region of Latin America, with approximately 6 million people infected [1]. Due to migration, parasite transmission in non-endemic countries has become an important health issue in the last years [2,3]. This pathogen has a complex life cycle that allows the passage from invertebrate to vertebrate hosts and vice versa, causing cardiac, digestive, neurological or mixed disorders in humans [4]. For survival, *T. cruzi* alternates between dividing and non-dividing forms. This is exerted by tight differentiation and cell cycle regulation mechanisms, which allow continuous adaptation to multiply in the two different hosts [5].

In eukaryotes, complexes formed by cyclins associated to cyclin-dependent kinases (cyclin–CDKs) are the main regulators of the cell cycle, assuring that the events of this process occur properly and unidirectional, resulting in the generation of two new daughter cells [6]. Different cyclin–CDK complexes phosphorylate specific key targets, triggering several downstream events [7]. In *Saccharomyces cerevisiae*, distinct cyclins are involved in several metabolic pathways [8,9]. Among those related to the cell cycle, various cyclin isoforms act at different phases of the cell cycle: G1-type cyclins are involved in initial bud formation and spindle pole duplication, S-type cyclins promote DNA replication and mitotic cyclins establish mitotic spindle orientation, allowing chromosome segregation [10]. Thus, cyclin specificity is required for proper cell cycle progression and this is achieved by different mechanisms [9]. For example, some cyclins are synthesized when they are required to activate CDKs, and then relocated or degraded when this activity needs to be diminished [11,12]. In mammalian cells, cyclin B associates and activates CDK1 to conform the mitosis-promoting factor, which phosphorylates substrates that are critical for entry into mitosis. By contrast, the destruction of cyclin B along with other factors promotes the exit from mitosis [13]. Several mitotic cyclins present a

* Corresponding author.
E-mail address: mariana.potenza@ingebi.conicet.gov.ar (M. Potenza).
[1] Present address: Institut Pasteur, Unité de Biologie cellulaire de l'infection microbienne, Paris, France; Centre National de la Recherche Scientifique, UMR 3691, Paris, France.

http://dx.doi.org/10.1016/j.parint.2015.12.007
1383-5769/© 2015 Elsevier Ireland Ltd. All rights reserved.

characteristic nine-amino-acid sequence known as destruction box (D-box), frequently located at the N-terminal site of the protein. This sequence targets the cyclin for rapid proteolysis via the anaphase-promoting complex, after its modification by the covalent addition of one or more ubiquitin molecules [14].

In *T. cruzi*, the mechanisms that regulate cell cycle are scarcely understood. Searches in the integrated TriTryp database [15] have shown that there are ten sequences carrying a typical cyclin box domain in the CL Brener *T. cruzi* genome [16,17]. Six of these sequences are closer to the PHO/PREG family of cyclins (*Tc*CYC2, *Tc*CYC4, *Tc*CYC5, *Tc*CYC7, *Tc*CYC10 and *Tc*CYC11), three of which have been functionally characterized by our group [17,18]. *Tc*CYC9 is similar to T-like cyclins, which are involved in transcriptional control in eukaryotes [19], whereas the remaining three (*Tc*CYC3, *Tc*CYC6 and *Tc*CYC8) show clear similarity with mitotic-type cyclins from other organisms. In this work, we characterized *Tc*CYC6, one of these mitotic sequences, and analyzed the phenotype of *T. cruzi* parasites that overexpress this protein fused to a nine amino acid tag from influenza virus hemagglutinin (*Tc*CYC6-HA).

2. Material andmethods

2.1. Sequence analysis

DNA sequences coding for putative cyclin 6 in the *T. cruzi* CL Brener genome were selected from the Kinetoplastid Genome Resource [15]. DNA and protein similarity were analyzed at the NCBI Blast server [20] and aligned using the NTI Vector 10 Advance software (Informax Inc., Bethesda). The GPS-ARM package software [21] was used for D-box motif identification.

2.2. Parasite cultures

T. cruzi epimastigote forms from the CL Brener clone and Tc. I Adriana [22,23] were used. Epimastigote cultures were grown at 28 °C in liver infusion tryptose medium (LIT) supplemented with 10% fetal bovine serum (FBS, Natocor), plus 10 U/ml penicillin and 10 mg/l streptomycin.

2.3. Transcription analysis of TcCYC6

Total RNA was isolated from *T. cruzi* epimastigotes using the Total RNA Extraction kit (Real Biotech Corporation), according to the manufacturer's instructions. cDNA was synthesized using 1 μg of RNA as template, M-MLV reverse transcriptase (Promega) and oligo-dT as primer in a 20 μl reaction. For the PCR step, 1 μl of a 1:10 dilution from the RT-reaction and primers CYC6_1 and CYC6_2 (Table 1) were used. Negative controls (to discard contaminant DNA) were performed with RNA samples without reverse transcription. PCR products were loaded onto 1% agarose gels and then purified for sequencing (Macrogen Inc.).

2.4. Tagging of the TcCYC6 sequence and cloning into the pTcINDEX vector

The *TcCYC6* coding region was amplified from genomic DNA by PCR using Pfu polymerase (New England Biolabs). A 1× hemagglutinin (HA) tag from human influenza virus was added to the C-terminal sequence by two rounds of consecutive PCRs using oligonucleotides CYC6_3, CYC6_4 and CYC6_5 (Table 1). The resulting *TcCYC6-HA* fusion sequence was cloned into the pZErO™-2 vector and amplified after transformation into the *Escherichia coli* DH5α strain (Invitrogen). *TcCYC6HA* was then subcloned into the *NotI–BamHI* sites of pTcINDEX vector [24].

Table 1
Oligonucleotides used in this study. Underlined letters in CYC6_3 and CYC6_5 indicate restriction sites for NotI and BamHI, respectively.

Oligo	Sequence 5′ → 3′
CYC6_1	GCATGAACTCCACAACACTGCGTGA
CYC6_2	GCTCAAGCGTAATCCGGAACGTCGT
CYC6_3	GCGGCCGCATGAACTCCACAACA
CYC6_4	AACGTCGTAGGGGTAGTCGACGT
CYC6_5	CGGATCCTCAAGCGTAATCCGGAACGT

2.5. Parasite transfections and protein expression

For inducible expression, the construct *pTcINDEX-TcCYC6-HA* was transfected into an epimastigote cell line containing the plasmid pLew13 [25], which expresses T7 RNA polymerase and tetracycline repressor genes. A standard electroporation method was used [23] and selection was allowed by growing parasites in the presence of 200 μg/ml Hygromycin B and 200 μg/ml Geneticin G418 (InvivoGen) for two months. Overexpression was induced with the addition of 5 μg/ml tetracycline (Sigma Aldrich). For controls, a culture overexpressing the enhanced green fluorescent protein (eGFP) under the same inducible system (kindly provided by Dr. J.J. Cazzulo, IIB-INTECH, Universidad Nacional de San Martín, Argentina) was used.

2.6. Preparation of protein extracts and western blot analysis

For preparation of total protein parasite extracts, 1×10^7 epimastigotes were harvested by centrifugation at 1000 ×*g* and disrupted with the addition of 5× SDS-PAGE loading buffer (5× SB). Clarified lysates and insoluble fractions from parasites were prepared as follows: 1×10^7 pelleted epimastigotes were resuspended in ice-cold PBS, disrupted by sonication (four pulses of 20 s each) and centrifuged at 20,000 ×*g* for 20 min. The fractions obtained (cytoplasmic supernatant and membranous pellet) were mixed separately with 5× SB in order to reach the same final volume for each sample. The different protein extracts were loaded onto 12% SDS-PAGE polyacrylamide gels and subjected to electrophoresis. Gels were transferred to nitrocellulose membranes and proteins detected using mouse monoclonal anti-HA (clone 16B12, Covance), mouse anti-β tubulin (Life Technologies), rabbit polyclonal anti-GFP or rabbit polyclonal anti-*Tc*Cyp19 antibodies (the last two kindly provided by Dr. Jaqueline Búa, ANLIS/Malbrán Institutes, Argentina). Horseradish peroxidase-conjugated goat anti-mouse or goat anti-rabbit IgGs (Calbiochem) were used as secondary antibodies. All antibodies were used at 1:1000 dilutions in 3% bovine serum albumin in PBS (BSA–PBS) and detected with ECL™ chemiluminescence kit (GE Healthcare), according to the manufacturer's instructions.

2.7. Immunofluorescence microscopy

T. cruzi epimastigotes overexpressing *Tc*CYC6-HA were spun down by centrifugation at 1000 ×*g* for 10 min, washed once in PBS and allowed to attach on poly-L-lysine-coated slides. Cells were fixed in 4% paraformaldehyde in PBS for 10 min, permeabilized with 0.1% Triton X-100 in PBS and washed twice with PBS. After blocking slides in 2% BSA–PBS, fixed parasites were incubated with anti-HA antibody, washed three times with PBS and then incubated with goat anti-mouse Alexa Fluor 594 antibody (Molecular Probes). Each antibody was diluted 1:1000 with 1% BSA–PBS and incubations were performed for 1 h at room temperature. Slides were mounted in ProLong Gold antifade reagent (Molecular Probes), containing 10 μg/mL of 4′,6′-diamino-2-phenylindole (DAPI). Cells were observed in an Olympus IX-71 inverted fluorescence microscope. Serial images of 0.2 μm (Z-increment) were acquired with a Hamamatsu R2 camera driven by Cell^R software (Olympus) and then processed by blind deconvolution using Autoquant X 2.1 software (Media Cybernetics).

2.8. Parasite growth curves

1×10^5 parasites/ml from *T. cruzi* cultures containing the p*Tc*INDEX-*TcCYC6-HA* or p*Tc*INDEX-eGFP constructions were grown in LIT medium in the presence or absence of tetracycline (5 μg/ml). Cultures were

incubated at 28 °C over time and 10 μl samples of each condition (with or without tetracycline for *Tc*CYC6-HA and eGFP-overexpressing cultures) were taken at 24-h intervals. The number of parasites was determined using a Neubauer chamber under an optical microscope. Samples were taken in triplicate and only motile cells were considered for counting. Statistical analysis was performed with two-factor ANOVA using Prism 5.00 software (GraphPad). Differences were considered significant at $p < 0.05$. Aliquots for each sample condition were also daily taken during 12 days for flow cytometry analysis as described in Section 2.10.

2.9. Parasite synchronization

T. cruzi epimastigotes containing the p*Tc*INDEX-*TcCYC6-HA* construction were induced or not with tetracycline for 48 h previous to synchronization with the addition of hydroxyurea, HU (Sigma Aldrich), as previously described [26]. Briefly, 1×10^6 parasites/ml were transferred to LIT media containing 20 mM HU and incubated at 28 °C for 24 h. Cell cycle was released by HU removal by washing the parasites three times with cold PBS and suspending them in fresh LIT medium with or without the addition of tetracycline (5 μg/ml). Samples were taken hourly at different time points spanning at least one complete round of the cell cycle and analyzed by flow cytometry as described below.

2.10. Flow cytometry analysis

Samples from Sections 2.8 to 2.9 were processed as follows: 6×10^6 cells were washed in PBS and fixed with 500 μL of 70% ethanol in PBS at 4 °C overnight. Fixed parasites were washed with PBS and incubated for 30 min at 37 °C with 500 μL of propidium iodide (PI) staining solution (2 mM EDTA, 10 mg/mL DNAse-free RNaseA and 20 mg/mL PI in PBS). Samples were analyzed in a flow cytometer (FACSAria, BD Biosciences) using the FACSDiva software. A total of 20,000 events were collected for each sample. Fluorescence intensity, which is proportional to the DNA content present in parasite populations, was plotted against cell number for each point to monitor the progression of cell cycle, using WinMDI 2.9 software. Experiments were carried out in independent triplicates.

2.11. Analysis of TcCYC6-HA turnover by proteasome inhibition assays

T. cruzi cultures containing the p*Tc*INDEX-*TcCYC6-HA* vector were induced by the addition of tetracycline (5 μg/ml) for 24 h. Subsequently, parasites were washed three times with phosphate buffer to remove the antibiotic. Cells were resuspended in the original volume of fresh LIT medium, divided into two bottles and incubated in the presence or absence of 100 μM MG132 (Z-Leu-Leu-Leu-al peptide) (Sigma Aldrich). For each condition, samples of 1 ml culture were taken at 24-h intervals after tetracycline removal, washed with PBS and prepared for western blot analysis by the addition of 5× SB.

3. Results

3.1. TcCYC6 belongs to the mitotic cyclin group and is transcribed in T. cruzi epimastigotes

Searches in the integrated TriTryp database [15] showed that *TcCYC6* is annotated as two sequences (TcCLB.511025.120 and TcCLB.507089.260) in the *T. cruzi* genome. These represent each single copy in the two homologous chromosomes, sharing 99% of positive matches. The coding sequence presents a cyclin box domain similar to mitotic regulator proteins from other trypanosomatids, plants and yeast (Fig. 1A). *Tc*CYC6 showed the highest similarity with cyclin 6 from *Trypanosoma brucei* and the putative cyclin 6 from *Leishmania brasiliensis* (66% and 75%, respectively). It also showed similarity with cyclin B from *Angomonas deanei* and cyclins from distant species such as *Daucus carota* (carrot) and *Physcomitrella patens* (moss), as well as with human cyclin B1.

RT-PCR performed with mature RNAs allowed the isolation of a 1100 bp-band that was identified by sequencing as the coding region for *TcCYC6*, confirming that this gene is actively transcribed in *T. cruzi* epimastigotes (Fig. 1B).

3.2. Recombinant TcCYC6-HA localizes along the cell body of T. cruzi

The inducible *Tc*CYC6-HA overexpression in *T. cruzi* was confirmed by western blot using the anti-HA antibody. A single band at the expected molecular weight was detected only when tetracycline was added to the parasite culture (Fig. 2A). Western blots containing separately the insoluble and soluble fractions of *T. cruzi* extracts showed *Tc*CYC6-HA mainly associated to the particulate fraction of the parasite cells (Fig. 2B). The same protein fractions were also analyzed with an anti-*Tc*Cyp19 antibody which detects the soluble protein cyclophilin 19 from *T. cruzi* [27], confirming proper disruption and separation of the two cellular fractions. To investigate *Tc*CYC6-HA distribution within the parasite cell, epimastigotes overexpressing *Tc*CYC6-HA were subjected to immunofluorescence microscopy. Transgenic parasites were induced with tetracycline, fixed on microscope slides and stained. We found that exogenous *Tc*CYC6-HA is localized along the cell body (Fig. 2C), without modifications at the different phases of the cell cycle (data not shown).

3.3. Overexpression of TcCYC6-HA is detrimental to epimastigotes

To analyze the phenotype of *Tc*CYC6-HA overexpressing parasites, growth curves were performed in the presence or absence of tetracycline to induce protein expression. Samples were taken until day 12 to assess cell proliferation by counting on a Neubauer chamber. The overexpression of *Tc*CYC6-HA inhibited the growth of *T. cruzi* epimastigotes in comparison to the same culture grown in the absence of tetracycline (Fig. 3A). On day 12, the concentration of *Tc*CYC6-HA overexpressing parasites decreased by 60%. A culture overexpressing eGFP under induction of tetracycline was used as control to discard any deleterious effect of the tetracycline addition or the induction of high protein levels on parasites. In this case, induced and non-induced cultures showed almost identical growth curves (Fig. 3A). The expressions of *Tc*CYC6-HA and eGFP were confirmed by western blot analysis (Fig. 3A, lower panels).

To analyze whether the cell cycle of the parasite could explain the growth arrest, we measured the DNA content of non-induced and *Tc*CYC6-HA overexpressing parasites by flow cytometry (Fig. 3B). Fixed samples of cultures growing in the presence or absence of tetracycline were taken until day 12, stained with IP and subjected to flow cytometry. The analysis showed that both cultures exhibited the typical histogram for an asynchronous cell population, with a major peak corresponding to parasites in G0/G1 phases (2C: 1 nucleus, 1 kinetoplast), and a smaller one representing cells at G2-mitosis boundary (4C: 2 nuclei, 2 kinetoplasts). However, a sub-G1 peak (1C) was distinguishable in *Tc*CYC6-HA overexpressing histograms from day 3, reaching 3.9% of the total population at day 12. This indicates the presence of an apoptotic and/or necrotic population as a result of cell cycle defects or cell death events.

To further study the effect of *Tc*CYC6-HA overexpression on each phase of the parasite cell cycle, transgenic epimastigotes were synchronized using HU and the cycle progression was analyzed at every hour. Fig. 3C shows the flow cytometry histograms at different times upon release of HU, for parasites which overexpress or not *Tc*CYC6-HA. At the point when HU was washed out (0 h), both populations, induced and non-induced, exhibited a major peak in G1 phase, in agreement with the HU treatment, which arrests the culture at this phase of the cycle [26]. After 8 h post-HU release, most non-induced parasites reached the S phase and then progressed through the cell cycle synchronically until to peak at the G2/M boundary (14 h). Since 18 h, the G1 peak

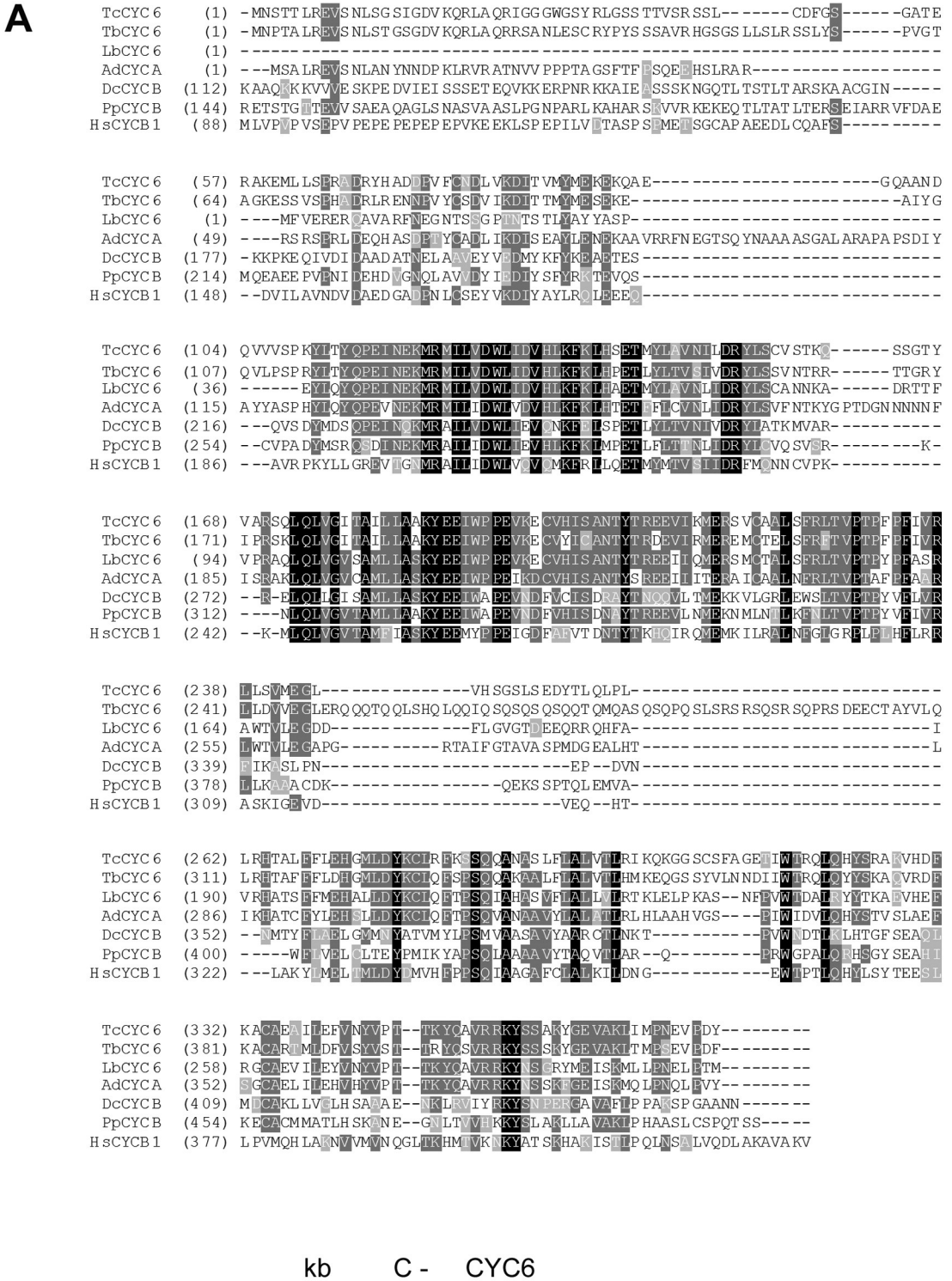

Fig. 1. Sequence analysis and transcription of *Tc*CYC6. (A) Multiple sequence alignment of the *Tc*CYC6 cyclin domain and those from other organisms: *Tb*CYC6 (*Trypanosoma brucei* CYC6, Tb927.11.16720), *Lb*CYC6 (putative CYC6, *Leishmania brasiliensis*, LbrM.32.3610), *Ad*CYCA (cyclin A from *Angomonas deanei*, EPY37545.1), *Dc*CYCB (cyclin B1–2 from carrot, *Daucus carota*, BAE72070.1), *Pp*CYCB (cyclin B1 from *Physcomitrella patens*, BAK64051.1) and *Hs*CYCB1 (human cyclin B1, *Homo sapiens*, EAW51306.1). Amino acid backgrounds are colored as follows: white for non-similar residues, black for identical residues, gray for conserved residues and light gray for similar residues. (B) Isolation of *TcCYC6* mRNA coding sequence. Agarose gel loaded with the RT-PCR reaction product used for subsequent sequencing (CYC6). Control reaction without reverse transcriptase (C−). kb: molecular marker size in kilobases.

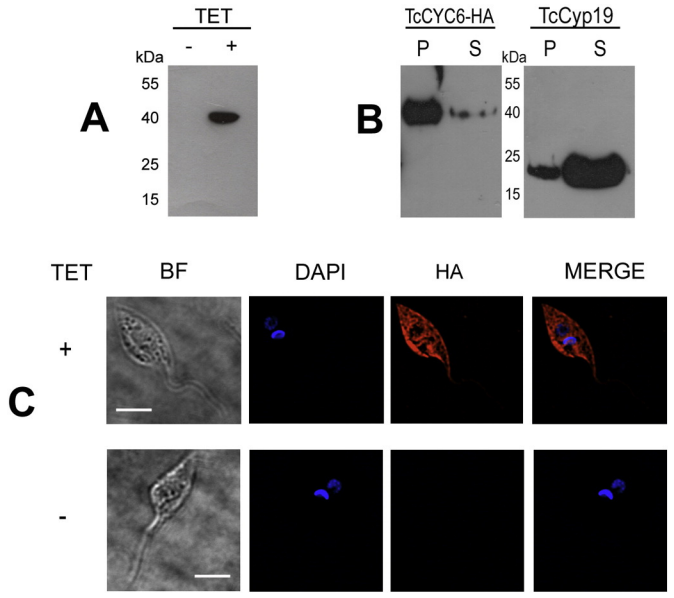

Fig. 2. Overexpression and localization of recombinant *Tc*CYC6-HA. (A) Western blot analysis of whole-cell extract from epimastigote cultures grown in the absence (−TET) or presence (+TET) of tetracycline. Protein induction was confirmed with the detection of a band signal at the expected size (44 kDa). (B) Protein extracts of *T. cruzi* were separated into insoluble pellet (P) and soluble lysate (S) fractions and then incubated with anti-HA or anti-*Tc*Cyp19 antibodies in a western blot to detect *Tc*CYC6-HA and *Tc*Cyp19 proteins, respectively. *Tc*CYC6-HA was found mainly in the insoluble fraction of protein parasite extracts. *Tc*Cyp19 was used as cell disruption control. (C) Localization of tagged *Tc*CYC6 in *T. cruzi*. An anti-HA antibody was used to detect the expression and localization of *Tc*CYC6HA in tetracycline-induced epimastigote cultures (+TET). BF, bright field; HA, anti-HA antibody staining; DAPI, staining of the nuclei and kinetoplast. Scale bar is indicated in the bright field, 5 μm.

reappeared in non-induced parasites, indicating the start of the next cycle. In contrast, parasites overexpressing *Tc*CYC6-HA did not reach major S or G2-phase single peaks as it was observed in control cells, maintaining a higher population of cells in G1 throughout the entire cycle. As it is showed in the insets of Fig. 3C, the lowest percentage of cells in G1-phase was 24% in parasites overexpressing *Tc*CYC6-HA, versus 2% found in the non-induced population. Note also that the percentage of the S-phase peak in *Tc*CYC6-HA-overexpressing cells was lower than the value observed for non-induced parasites (58% versus 90%, respectively). This result suggests that the entrance into S phase (or the G1/S transition) is impaired when *Tc*CYC6-HA is overexpressed in *T. cruzi* epimastigotes.

3.4. Degradation of overexpressed TcCYC6-HA in epimastigotes

Searches for conserved motifs revealed the presence of two putative D-boxes at residues 3 and 44 in *Tc*CYC6, whose sequences are STTLREVSN and RSSLRDFGS, respectively (Fig. 4A). These domains showed different levels of identity with, and are at similar position as, the D-boxes present in *Tb*CYC6 from *T. brucei* and in human mitotic cyclins B1 and A2 (Fig. 4B).

To investigate the turnover of *Tc*CYC6-HA in vivo, *T. cruzi* cultures were grown in the presence of tetracycline for 24 h to induce expression and then the antibiotic was removed to prevent more protein synthesis. After tetracycline removal, parasites were treated or not with the proteasome inhibitor MG132 and the presence of tagged *Tc*CYC6 was determined by western blot using the anti-HA antibody (Fig. 4C, upper panels). In the presence of the inhibitor, *Tc*CYC6-HA was detected in all samples analyzed at similar amounts. By contrast, in the absence of MG132 the intensity of the protein band was weaker after 3 days and undetectable in samples taken 8 days after tetracycline removal, indicating rapid turnover. As *T. cruzi* stops growing in the presence of proteasome inhibitors [28,29], constant volumes of samples and not constant number of cells were collected to correct the decrease in *Tc*CYC6-HA concentration due to the dilution of the protein caused by cell proliferation. The same western blots revealed with an anti-tubulin antibody showed the presence of a greater number of cells in the untreated culture, confirming that the decrease of *Tc*CYC6-HA in this culture is due to proteasoma turnover and not to dilution caused by cell proliferation (Fig. 4C, lower panels).

4. Discussion

In this report, we studied the effect of the overexpression of a sequence coding for a putative mitotic cyclin on *T. cruzi* epimastigotes. Cell counting showed that parasite growth decreased after induction of HA-tagged *Tc*CYC6. Control cultures overexpressing eGFP were included to discard side effects due to tetracycline or non-physiological protein levels on parasite proliferation. In this regard, cultures expressing eGFP showed the same growth curve as controls, confirming the detrimental effect of *Tc*CYC6-HA overexpression on *T. cruzi*.

Searches in databases and alignment analysis showed that *Tc*CYC6 is closely related to the mitotic cyclin 6 from *T. brucei*, *Tb*CYC6. RNA interference-mediated silencing of this gene produced a mitotic block in both the bloodstream and procyclic forms of *T. brucei* [30,31], but no phenotypic analysis is available on the overexpression of *Tb*CYC6. Here, the cell cycle profile of asynchronous *Tc*CYC6-HA-overexpressing parasites showed no changes in comparison with non-induced cultures, regarding to the relative proportions of cultures in each G0/G1, S or G2/M phases or a cell cycle arrest. However, the phenotype of both population of parasites synchronized with hydroxyurea revealed that the G1/S transition was affected by the overexpression of *Tc*CYC6-HA. We found that in induced cells, there was a proportion of the population unable to exit from G1 and enter into the S-phase. This was evidenced by the presence of higher percentages of cells in G1 throughout the entirely cell cycle for *Tc*CYC6-HA-overexpressing parasites compared to non-induced cells. Even within a clonal population, it has been reported that protein overexpression levels can vary in cells when using the pTcINDEX system [24]. This may be the case for *Tc*CYC6-HA-overexpressing parasites: the G1/S transition could be seriously compromised in those cells expressing high levels of *Tc*CYC6-HA; meanwhile the rest of the culture, expressing lower quantities of the fusion protein, would exhibit a phenotype more resembling to non-induced parasites. In fact, a cell cycle with a less efficient G1/S transition could contribute to the appearance of the slight sub-G1 peak observed in asynchronous *Tc*CYC6-HA-induced parasites (Fig. 3B). One explanation for the cell cycle defects at the G1/S transition exerted by the overexpression of a mitotic-type cyclin might be due to sequestration and inactivation of essential CDKs necessary to the successful entrance into the S phase. On the other hand, localization of *Tc*CYC6-HA by immunofluorescence microscopy showed this protein throughout the parasite cell body, but western blot analysis of *T. cruzi* protein extracts showed that *Tc*CYC6-HA was expressed at high levels, mainly associated with the insoluble

Fig. 3. Analysis of *Tc*CYC6-HA overexpressing parasites. (A) Growth curves of parasites overexpressing *Tc*CYC6-HA or eGFP proteins. The figure shows the proliferation of epimastigote cultures in the presence or absence of tetracycline (+TET or −TET, respectively). The number of cells was determined by counting on a microscope and plotted against incubation time (*Days*), for both cultures overexpressing *Tc*CYC6-HA or eGFP (control curves). One asterisk (*) indicates $p < 0.05$ and three asterisks (***), $p < 0.001$ evaluated by two-factor ANOVA. Below each curve, a western blot analysis is shown for the detection of overexpressed proteins, *Tc*CYC6-HA and eGFP, using anti-HA and anti-GFP antibodies, respectively. Numbers 1 to 12: days of cell counting. (B) Flow cytometry analysis of *T. cruzi* epimastigotes in the presence (+TET) or absence (−TET) of tetracycline over time. Histograms from a representative experiment with samples taken 1, 3, 5, 8 and 12 days after *Tc*CYC6-HA induction are shown. (C) Flow cytometry analysis of HU-synchronized epimastigotes in the presence (+TET) or absence (−TET) of tetracycline over an entire cell cycle. The figure shows a representative experiment with histograms for samples taken at 0, 8, 14, 18, 20 and 24 h post-HU release. For B and C, histogram insets show the percentages of population in sub-G1, G0/G1, G1, S or G2/M phases.

fraction. Thus, the inability to produce a rapid *Tc*CYC6-HA clearance by the parasite could also contribute to cellular death. It is also worth noting that we failed to obtain the recombinant *Tc*CYC6-HA from an expression system based in *E. coli*, probably due to growth arrest after induction of protein expression (data not shown). Altogether, these data suggest that high amounts of this putative cyclin inside the cell,

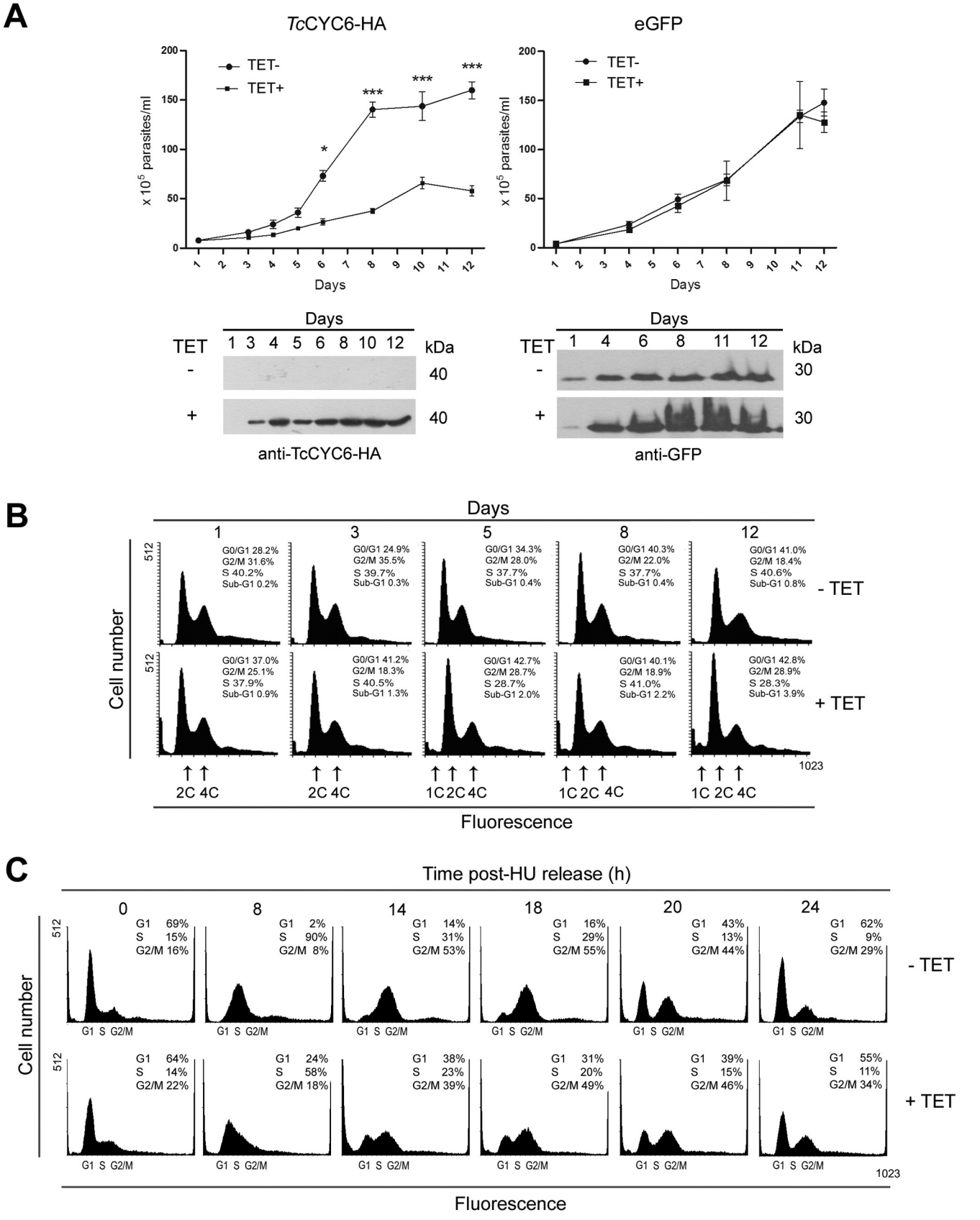

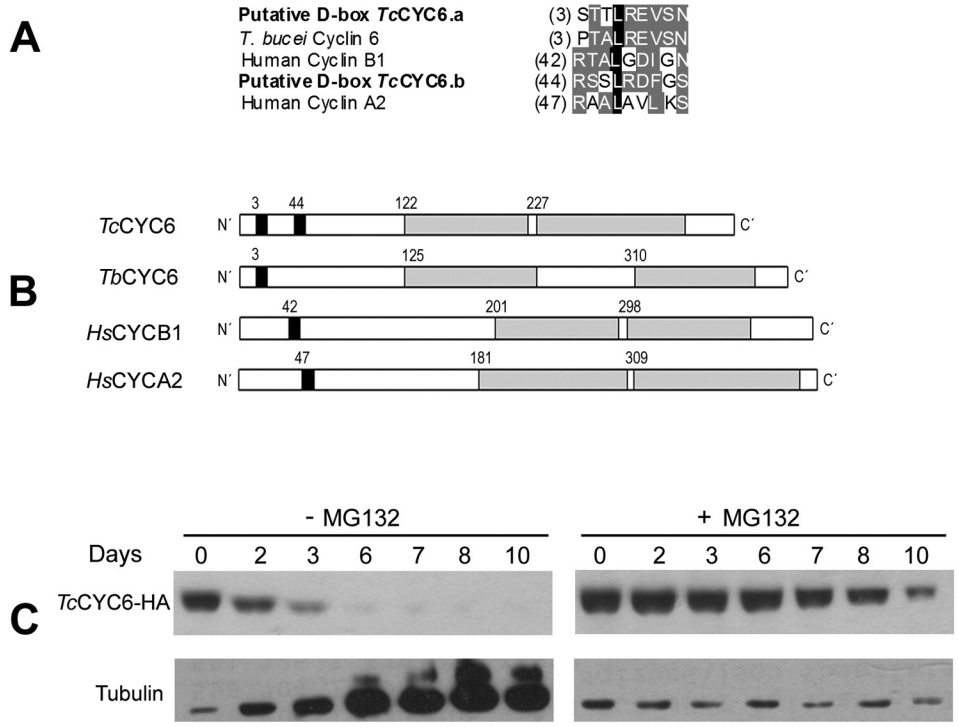

Fig. 4. D-box prediction and turnover of *Tc*CYC6-HA. (A) Alignment of putative D-boxes at positions 3 (*Tc*CYC6.a) and 44 (*Tc*CYC6.b) on *Tc*CYC6 with those from *T. brucei* CYC6 and human cyclins B1 and A2 (accession numbers Tb927.11.16720, EAW51306.1 and EAX05246.1, respectively). Black and gray amino acid backgrounds indicate identical and conserved residues, respectively. (B) Schematic representation and localization of D-boxes from *Tc*CYC6 and its orthologues. Numbers above boxes indicate amino acid positions. Black and light gray boxes represent D-box and cyclin box domains, respectively. N′ and C′ refer to N- and C-termini of protein sequences. (C) Turnover of *Tc*CYC6-HA. Samples of protein extracts from epimastigote cultures grown in the presence or absence of MG132 were analyzed by western blot. Anti-HA antibodies were used for the detection of *Tc*CYC6-HA (upper panels) and anti-tubulin antibodies were used as protein loading control (lower panels). Numbers 0 to 10: samples taken at days after tetracycline removal.

far higher than its physiological levels, produce toxic effects to the cell and also alter the cell cycle at G1/S transition.

As the experiments shown here were performed on the base of recombinant *Tc*CYC6-HA, it is valid to ask whether the endogenous gene becomes in fact translated and therefore whether it is present as a protein inside the parasite. First, we analyzed whether this gene is transcribed, assessing the presence of mRNA coding for the *Tc*CYC6 sequence. Results from RT-PCRs and sequencing confirmed that this gene is present as a mature transcript in *T. cruzi* epimastigotes. However, polyclonal antibodies raised against the N-terminus of *Tc*CYC6 failed to detect the protein in western blots of *T. cruzi* extracts (data not shown), although kinase activity could be observed in the immunoprecipitated protein complex (Supplementary material 1). This could indicate that, if expressed, *Tc*CYC6 is present in the parasite but at very short specific points along the cell cycle or at quantities too low to be detected by western blot or any indirect method. To our knowledge, the presence of this protein is still undetectable by the proteomic initiatives [32–50]. These findings support the idea that *Tc*CYC6 functions as a regulatory protein, with a tightly regulated expression. This could be the reason why overexpressing *Tc*CYC6 protein over the physiological levels was detrimental to parasite growth. It is important to consider that the observed effects of *Tc*CYC6-HA overexpression on *T. cruzi* could also be unspecific. This may occur due to coaggregation of *Tc*CYC6-HA with unrelated proteins, although experimentation to explore this hypothesis requires proteome-wide analysis.

The HA epitope has been previously successfully used to tag sequences in trypanosomatid parasites [51,52] including *T. cruzi*, using constitutive [17,53] or inducible [23] expression systems. This background suggests that the deleterious effect on epimastigotes is due to the *Tc*CYC6 sequence itself, rather than to the HA tag.

The presence of a short sequence called D-box is a hallmark for cyclins involved in mitotic controls. In eukaryotic cells, mitotic cyclins can be modified with the addition of one or multiple subunits of ubiquitin, in a process called poly-ubiquitination [14]. This modification triggers the degradation of ubiquitinated proteins by the proteasome, a complex of multiprotein cylindrical structures composed of several proteases, reviewed by [54]. In the cell cycle, cyclin degradation is a crucial event in exiting metaphase and entering the next cell cycle [55,56]. This mechanism of ubiquitin proteasome pathway for regulation of cyclin concentration within the cell is also present in trypanosomatids such as *T. brucei* [57]. Here, we showed that *Tc*CYC6 has two nine amino acid domains at its N-terminal sequence, similar to a destruction box (D-box). These motifs present divergence from the consensus sequence found in other organisms [58], although one of them is 78% identical to its ortholog in *T. brucei*, the mitotic cyclin 6 [30,31]. To assess the importance of the putative D-box motifs on the *Tc*CYC6-HA turnover, we analyzed the level of this protein in the presence or absence of a proteasome inhibitor (MG132) after a pulse of tetracycline addition. Western blots of parasite extracts detected *Tc*CYC6-HA in samples collected at 2 and 3 days after tetracycline removal in the absence of MG132, meanwhile it was present in those taken up to 10 days in the presence of the inhibitor, suggesting rapid degradation of this protein in vivo. In this experiment, parasite extracts from cultures overexpressing eGFP were unsuitable as degradation control due to basal protein expression, even in the absence of tetracycline (Fig. 3A). Leaky expression of fluorescent proteins in un-induced parasites has been found previously [59], specially with those non-toxic proteins. However, the result presented here is a first approach to assess the role of proteasome in the degradation of *Tc*CYC6 and mutational analysis on its putative D-boxes is under way to confirm this hypothesis.

The cyclin function of *Tb*CYC6 from *T. brucei* was assayed by Hammarton et al. [30]. In this regard, it was showed that the cyclin box domain of *Tb*CYC6 restored the growth arrest in a complementation assay using the DL1 *S. cerevisiae* strain. This mutant yeast harbors a cyclin G1 deficiency [60] but has been used to identify and characterize both G1/S [61] and G2/M cyclins [62]. This means that the growth arrest

of *S. cerevisiae* DL1 can be rescued by different types of cyclins. We studied the cyclin function of *Tc*CYC6-HA using the same complementation assay, but this sequence was unable to rescue the lethal phenotype of DL1 strain (data not shown). The belonging of *Tc*CYC6 to the mitotic-type cyclins could not be the reason why it failed to complement the cyclin function and rescue the growth arrest. Instead, experiments using only the cyclin domain should be performed to confirm or discard the cyclin function.

In summary, our results provide evidence that *Tc*CYC6 is transcribed in *T. cruzi* epimastigotes but also that its overexpression affects the cell cycle of the parasite. The pathways and function of this protein with homology to mitotic cyclins exerted on *T. cruzi* are not yet elucidated and deserve more research. The data presented here suggest that *Tc*CYC6 is subjected to a strong gene expression regulation.

Conflict of interest

The authors declare that they have no conflict of interest.

Acknowledgments

We thank Dr. Jaqueline Búa for the anti-*Tc*Cyp19 and anti-GFP antibodies and Dr. J.J. Cazzulo for the p*Tc*INDEX-eGFP *T. cruzi* cell line. We thank John Kelly and Martin Taylor (London School of Tropical Medicine, London, UK) for kindly providing the p*Tc*INDEX vector. This work was supported by grants from the Consejo Nacional de Investigaciones Científicas y Técnicas (CONICET, PIP 112-201101-00924), the Agencia Nacional de Promoción científica y Tecnológica (ANPCyT, PICT 2010-0140) and the AMSUD-PASTEUR Training Program for Young Investigators. ML had fellowships from AMSUD-PASTEUR, ANPCyT and CONICET. His work was done in the laboratory of Dr. J.J. Cazzulo (Instituto de Investigaciones Biotecnológicas IIB-INTECH). MP and MTTI are members of the Research Career of CONICET.

Appendix A. Supplementary data

Supplementary data to this article can be found online at http://dx.doi.org/10.1016/j.parint.2015.12.007.

References

[1] World Health Organization, Chagas Disease (American Trypanosomiasis), 2015 (Fact sheet No. 340 www.who.int/mediacentre/factsheets/fs340. Last accessed November 19th).
[2] F. Gobbi, A. Angheben, M. Anselmi, C. Postiglione, E. Repetto, D. Buonfrate, S. Marocco, S. Tais, A. Chiampan, P. Mainardi, Z. Bisoffi, Profile of *Trypanosoma cruzi* infection in a tropical medicine reference center, Northern Italy, PLoS Negl. Trop. Dis. 8 (2014), e3361.
[3] A. Assal, C. Corbi, Chagas disease and blood transfusion: an emerging issue in non-endemic countries, Transfus. Clin. Biol. 18 (2011) 286–291.
[4] A.R. Teixeira, N. Nitz, M.C. Guimaro, C. Gomes, C.A. Santos-Buch, Chagas disease, Postgrad. Med. J. 82 (2006) 788–798.
[5] K.M. Tyler, D.M. Engman, The life cycle of *Trypanosoma cruzi* revisited, Int. J. Parasitol. 31 (2001) 472–481.
[6] H. Harashima, N. Dissmeyer, A. Schnittger, Cell cycle control across the eukaryotic kingdom, Trends Cell Biol. 23 (2013) 345–356.
[7] H. Hochegger, S. Takeda, T. Hunt, Cyclin-dependent kinases and cell-cycle transitions: does one fit all? Nat. Rev. Mol. Cell Biol. 9 (2008) 910–916.
[8] K. Huang, I. Ferrin-O'Connell, W. Zhang, G.A. Leonard, E.K. O'Shea, F.A. Quiocho, Structure of the Pho85–Pho80 CDK–cyclin complex of the phosphate-responsive signal transduction pathway, Mol. Cell 28 (2007) 614–623.
[9] J. Bloom, F.R. Cross, Multiple levels of cyclin specificity in cell-cycle control, Nat. Rev. Mol. Cell Biol. 8 (2007) 149–160.
[10] M.D. Mendenhall, A.E. Hodge, Regulation of Cdc28 cyclin-dependent protein kinase activity during the cell cycle of the yeast *Saccharomyces cerevisiae*, Microbiol. Mol. Biol. Rev. 62 (1998) 1191–1243.
[11] J. Pines, T. Hunter, Human cyclins A and B1 are differentially located in the cell and undergo cell cycle-dependent nuclear transport, J. Cell Biol. 115 (1991) 1–17.
[12] D.H. Parry, G.R.X. Hickson, P.H. O'Farrell, Cyclin B destruction triggers changes in kinetochore behavior essential for successful anaphase, Curr. Biol. 13 (2003) 647–653.
[13] F. Chesnel, F. Bazile, A. Pascal, J.Z. Kubiak, Cyclin B dissociation from CDK1 precedes its degradation upon MPF inactivation in mitotic extracts of *Xenopus laevis* embryos, Cell Cycle 5 (2006) 1687–1698.
[14] M. Glotzer, A.W. Murray, M.W. Kirschner, Cyclin is degraded by the ubiquitin pathway, Nature 349 (1991) 132–138.
[15] The Kinetoplastid Genome Resource, http://tritrypdb.org/tritrypdb/2015 (Last accessed May 15th).
[16] N.M. El-Sayed, P.J. Myler, D.C. Bartholomeu, D. Nilsson, G. Aggarwal, A.N. Tran, E. Ghedin, E.A. Worthey, A.L. Delcher, G. Blandin, S.J. Westenberger, et al., The genome sequence of *Trypanosoma cruzi*, etiologic agent of Chagas disease, Science 309 (2005) 409–415.
[17] M. Potenza, S. Schenkman, M. Laverrière, M.T. Tellez-Inon, Functional characterization of *Tc*CYC2 cyclin from *Trypanosoma cruzi*, Exp. Parasitol. 132 (2012) 537–545.
[18] E.B. Gómez, M.I. Santori, S. Laria, J.C. Engel, J. Swindle, H. Eisen, P. Szankasi, M.T. Tellez-Iñión, Characterization of the *Trypanosoma cruzi* Cdc2p related protein kinase 1 and identification of three novel associating cyclins, Mol. Biochem. Parasitol. 113 (2001) 97–108.
[19] A. De Luca, M. De Falco, A. Baldi, M.G. Paggi, Cyclin T: three forms for different roles in physiological and pathological functions, J. Cell. Physiol. 194 (2003) 101–107.
[20] S.F. Altschul, W. Gish, W. Miller, E.W. Myers, D.J. Lipman, Basic local alignment search tool, J. Mol. Biol. 215 (1990) 403–410.
[21] Z. Liu, F. Yuan, J. Ren, J. Cao, Y. Zhou, Q. Yang, Y. Xue, GPS-ARM: computational analysis of the APC/C recognition motif by predicting D-boxes and KENBoxes, PLoS One 7 (2012), e34370.
[22] I. Urban, L.B. Santurio, A. Chidichimo, H. Yu, X. Chen, J. Mucci, F. Agüero, C.A. Buscaglia, Molecular diversity of the *Trypanosoma cruzi Tc*SMUG family of mucin genes and proteins, Biochem. J. 438 (2011) 303–313.
[23] M. Laverrière, J.J. Cazzulo, V.E. Alvarez, Antagonic activities of *Trypanosoma cruzi* metacaspases affect the balance between cell proliferation, death and differentiation, Cell Death Differ. 19 (2012) 1358–1369.
[24] M.C. Taylor, J.M. Kelly, pTcINDEX: a stable tetracycline-regulated expression vector for *Trypanosoma cruzi*, BMC Biotechnol. 6 (2006) 32.
[25] E. Wirtz, S. Leal, C. Ochatt, G.A. Cross, A tightly regulated inducible expression system for conditional gene knock-outs and dominant-negative genetics in *Trypanosoma brucei*, Mol. Biochem. Parasitol. 99 (1999) 89–101.
[26] N. Galanti, J.A. Dvorak, J. Grenet, J.P. McDaniel, Hydroxyurea-induced synchrony of DNA replication in the kinetoplastida, Exp. Cell Res. 214 (1994) 225–230.
[27] J. Búa, L. Aslund, N. Pereyra, G.A. García, E.J. Bontempi, A.M. Ruiz, Characterisation of a cyclophilin isoform in *Trypanosoma cruzi*, FEMS Microbiol. Lett. 200 (2001) 43–47.
[28] J.P. da Cunha, E.S. Nakayasu, M.C. Elias, D.C. Pimenta, M.T. Tellez-Iñón, F. Rojas, M.J. Muñoz, I.C. Almeida, S. Schenkman, *Trypanosoma cruzi* histone H1 is phosphorylated in a typical cyclin dependent kinase site accordingly to the cell cycle, Mol. Biochem. Parasitol. 140 (2005) 75–86.
[29] J. Cardoso, M.J. Soares, R.F. Menna-Barreto, R. Le Bloas, V. Sotomaior, S. Goldenberg, M.A. Krieger, Inhibition of proteasome activity blocks *Trypanosoma cruzi* growth and metacyclogenesis, Parasitol. Res. 103 (2008) 941–951.
[30] T.C. Hammarton, J. Clark, F. Douglas, M. Boshart, J.C. Mottram, Stage-specific differences in cell cycle control in *Trypanosoma brucei* revealed by RNA interference of a mitotic cyclin, J. Biol. Chem. 278 (2003) 22877–22886.
[31] Z. Li, C.C. Wang, A PHO80-like cyclin and a B-type cyclin control the cell cycle of the procyclic form of *Trypanosoma brucei*, J. Biol. Chem. 278 (2003) 20652–20658.
[32] J.A. Atwood, D.B. Weatherly, T.A. Minning, B. Bundy, C. Cavola, F.R. Opperdoes, R. Orlando, R.L. Tarleton, The *Trypanosoma cruzi* proteome, Science 309 (2005) 473–476.
[33] M.J. Ayub, J. Atwood, A. Nuccio, R. Tarleton, M.J. Levin, Proteomic analysis of the *Trypanosoma cruzi* ribosomal proteins, Biochem. Biophys. Res. Commun. 382 (2009) 30–34.
[34] S.A. Kikuchi, C.L. Sodre, D.E. Kalume, C.G.R. Elias, A.L.S. Santos, S.M. de Nazare, M. Meuser, A. Chapeaurouge, J. Perales, O. Fernandes, Proteomic analysis of two *Trypanosoma cruzi* zymodeme 3 strains, Exp. Parasitol. 126 (2010) 540–551.
[35] C. Sant'Anna, E.S. Nakayasu, M.G. Pereira, D. Lourenço, W. de Souza, I.C. Almeida, N.L. Cunha-e-Silva, Subcellular proteomics of *Trypanosoma cruzi* reservosomes, Proteomics 9 (2009) 1782–1794.
[36] P.N. Ulrich, V. Jimenez, M. Park, V.P. Martins, J. Atwood, K. Moles, D. Collins, P. Rohloff, R. Tarleton, S.N.J. Moreno, R. Orlando, R. Docampo, Identification of contractile vacuole proteins in *Trypanosoma cruzi*, PLoS One 6 (2011), e18013.
[37] R.M. Queiroz, S. Charneau, I.M. Bastos, J.M. Santana, M.V. Sousa, P. Roepstorff, C.A. Ricart, Cell surface proteome analysis of human-hosted *Trypanosoma cruzi* life stages, J. Proteome Res. 13 (2014) 3530–3541.
[38] E. Bayer-Santos, C. Aguilar-Bonavides, S.P. Rodrigues, E.M. Cordero, A.F. Marques, A. Varela-Ramirez, H. Choi, N. Yoshida, J.F. da Silveira, I.C. Almeida, Proteomic analysis of *Trypanosoma cruzi* secretome: characterization of two populations of extracellular vesicles and soluble proteins, J. Proteome Res. 12 (2013) 883–897.
[39] E.M. Cordero, E.S. Nakayasu, L.G. Gentil, N. Yoshida, I.C. Almeida, J.F. da Silveira, Proteomic analysis of detergent-solubilized membrane proteins from insect-developmental forms of *Trypanosoma cruzi*, J. Proteome Res. 8 (2009) 3642–3652.
[40] M. Ferella, D. Nilsson, H. Darban, C. Rodrigues, E.J. Bontempi, R. Docampo, B. Andersson, Proteomics in *Trypanosoma cruzi* — localization of novel proteins to various organelles, Proteomics 8 (2008) 2735–2749.
[41] J. Paba, C.A.O. Ricart, W. Fontes, J.M. Santana, A.R.L. Teixeira, J. Marchese, B. Williamson, T. Hunt, B.L. Karger, M.V. Sousa, Proteomic analysis of *Trypanosoma cruzi* developmental stages using isotope-coded affinity tag reagents, J. Proteome Res. 3 (2004) 517–524.
[42] J. Paba, J.M. Santana, A.R.L. Teixeira, W. Fontes, M.V. Sousa, C.A.O. Ricart, Proteomic analysis of the human pathogen *Trypanosoma cruzi*, Proteomics 4 (2004) 1052–1059.

[43] C. Sodré, A. Chapeaurouge, D. Kalume, L.L. de Mendonca, J. Perales, O. Fernandes, Proteomic map of *Trypanosoma cruzi* CL Brener: the reference strain of the genome project, Arch. Microbiol. 191 (2009) 177–184.
[44] H.G. Vieira, P. Grynberg, M. Bitar, F. Pires Sda, H.O. Hilário, A.M. Macedo, C.R. Machado, H.M. de Andrade, G.R. Franco, Proteomic analysis of *Trypanosoma cruzi* response to ionizing radiation stress, PLoS One 9 (2014), e97526.
[45] D. Pérez-Morales, H. Lanz-Mendoza, G. Hurtado, R. Martínez-Espinosa, B. Espinoza, Proteomic analysis of *Trypanosoma cruzi* epimastigotes subjected to heat shock, J. Biomed. Biotechnol. 2012 (2012) 902803.
[46] F.K. Marchini, L.M. de Godoy, R.C. Rampazzo, D.P. Pavoni, C.M. Probst, F. Gnad, M. Mann, M.A. Krieger, Profiling the *Trypanosoma cruzi* phosphoproteome, PLoS One 6 (2011), e25381.
[47] A.D. Magalhães, S. Charneau, J. Paba, R.A. Guércio, A.R. Teixeira, J.M. Santana, M.V. Sousa, C.A. Ricart, *Trypanosoma cruzi* alkaline 2-DE: optimization and application to comparative proteome analysis of flagellate life stages, Proteome Sci. 6 (2008) 24.
[48] A.D. Magalhães, R.M. Queiroz, I.M. Bastos, J.M. Santana, M.V. Sousa, C.A. Ricart, S. Charneau, Comparative two-dimensional gel electrophoresis of *Trypanosoma cruzi* mammalian-stage forms in an alkaline pH range, Protein Pept. Lett. 22 (2015) 1066–1075.
[49] C. Santos Júnior Ade, D.E. Kalume, R. Camargo, D.P. Gómez-Mendoza, J.R. Correa, S. Charneau, M.V. Sousa, B.D. Lima, C.A. Ricart, Unveiling the *Trypanosoma cruzi* nuclear proteome, PLoS One 10 (2015), e0138667.
[50] L.M. de Godoy, F.K. Marchini, D.P. Pavoni, C. Rampazzo Rde, C.M. Probst, S. Goldenberg, M.A. Krieger, Quantitative proteomics of *Trypanosoma cruzi* during metacyclogenesis, Proteomics 12 (2012) 2694–2703.
[51] M.M. Pereira, A.M. Malvezzi, L.M. Nascimento, T.D. Lima, V.S. Alves, M.L. Palma, E.R. Freire, D.M. Moura, C.R. Reis, O.P. de Melo Neto, The eIF4E subunits of two distinct trypanosomatid eIF4F complexes are subjected to differential post-translational modifications associated to distinct growth phases in culture, Mol. Biochem. Parasitol. 190 (2013) 82–86.
[52] J. Týc, S. Long, M. Jirků, J. Lukes, YCF45 protein, usually associated with plastids, is targeted into the mitochondrion of *Trypanosoma brucei*, Mol. Biochem. Parasitol. 173 (2010) 43–47.
[53] P.A. Haynes, D.G. Russell, G.A. Cross, Subcellular localization of *Trypanosoma cruzi* glycoprotein Gp72, J. Cell Sci. 109 (1996) 2979–2988.
[54] S. Bhattacharyya, H. Yu, C. Mim, A. Matouschek, Regulated protein turnover: snapshots of the proteasome in action, Nat. Rev. Mol. Cell Biol. 15 (2014) 122–133.
[55] H. Yamano, C. Tsurumi, J. Gannon, T. Hunt, The role of the destruction box and its neighbouring lysine residues in cyclin B for anaphase ubiquitin-dependent proteolysis in fission yeast: defining the D-box receptor, EMBO J. 17 (1998) 5670–5678.
[56] V. Sudakin, D. Ganoth, A. Dahan, H. Heller, J. Hershko, F.C. Luca, J.V. Ruderman, A. Hershko, The cyclosome, a large complex containing cyclin-selective ubiquitin ligase activity, targets cyclins for destruction at the end of mitosis, Mol. Biol. Cell 6 (1995) 185–197.
[57] J.J. Van Hellemond, J.C. Mottram, The CYC3 gene of *Trypanosoma brucei* encodes a cyclin with a short half-life, Mol. Biochem. Parasitol. 111 (2000) 275–282.
[58] T. Jadhav, M.W. Wooten, Defining an embedded code for protein ubiquitination, J. Proteomics. Bioinform. 2 (2009) 316.
[59] V.L. Alonso, C. Ritagliati, P. Cribb, E.C. Serra, Construction of three new Gateway® expression plasmids for *Trypanosoma cruzi*, Mem. Inst. Oswaldo Cruz 109 (2014) 1081–1085.
[60] D.J. Lew, V. Duli, S.I. Reed, Isolation of three novel human cyclins by rescue of G1 cyclin (cln) function in yeast, Cell 66 (1991) 1197–1206.
[61] H.E. Richardson, L.V. O'Keefe, S.I. Reed, R. Saint, A *Drosophila* G1-specific cyclin E homolog exhibits different modes of expression during embryogenesis, Development 119 (1993) 673–690.
[62] I.S. Day, A.S. Reddy, M. Golovkin, Isolation of a new mitotic-like cyclin from *Arabidopsis*: complementation of a yeast cyclin mutant with a plant cyclin, Plant Mol. Biol. 30 (1996) 565–575.